

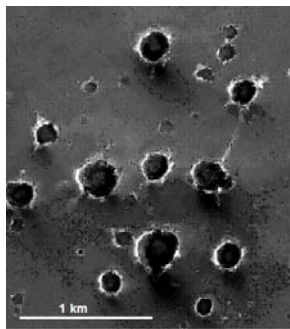
## SMALL PRIMARIES VERSUS LARGE SECONDARIES ON MARS – NUMERICAL APPROACH.

N. Artemieva, Institute for Dynamics of Geospheres, Moscow, artemeva@psi.edu

**Introduction:** Recent data on small martian craters revert scientists to a serious problem discussed by Shoemaker [1] 40 years ago: are small (less than ~1 km diameter) craters dominated by primary impacts, by secondary impacts of much larger primary craters, or are both the primaries and the secondaries significant [2,3]? In this paper we use numerical approach to model small primary clustered craters, created by disrupted and dispersed projectiles; and high-velocity ejecta from km-sized craters which produce distal craters probably indistinguishable from small primaries.

**Numerical methods:** We model atmospheric entry of small asteroids, impact cratering, and high-velocity impact ejecta motion using three dimensional hydrocode SOVA [4] complemented by a proper equation of state for basalt [5]. We use a tracer (massless) particle technique to reconstruct dynamic (trajectories, velocities), thermodynamic (pressure, temperature) and disruption (strain, strain rate) histories in any part of the flow. The motion of ejecta in the post-impact plume is described in the frame of two-phase hydrodynamics: every ejected fragment is characterized by its individual parameters (mass, density, position, and velocity) and exchanges momentum and energy with surrounding vapor-air mixture. Details of the model may be found in the recently published paper [6].

We also use simplified approach, separated fragment model [7,8] to study disruption of stony and iron asteroids in a modern martian atmosphere.



In contrast to the more common ‘pancake’ model [9], which treats the disrupted meteoroid as a deformable (but continuous) liquid, our approximation enables us to define the mass-velocity distribution on the surface for solid fragments which create a single crater or a group of craters (in the case of high final velocity) or which may be found as meteorites (fragments with low final velocity).

**Strewn fields on Mars:** Strewn fields are created by projectiles with a mass approximately equal to the mass of atmosphere in a “trajectory tube” (a cylinder with length equal to the trajectory length and radius equal to the projectile radius). Extrapolating to modern martian atmosphere we find that iron projectiles with mass as low as  $10^3$ - $10^4$  kg are not disrupted on Mars at

all! Stony projectiles with the mass in the range of  $10^4$ - $10^5$  are disrupted and may produce crater fields with weak separation, which may be identified most probably as irregular craters sized ~100 m (too small to be recognized in details even by the MOC MGS). Nevertheless this camera revealed a lot of crater fields with typical crater size of 0.2-1 km and separation of ~1 km (**Fig.1**). Assuming atmospheric dispersion nature of these clusters we need high-velocity, extremely low-density ( $0.015 \text{ g/cm}^3$ ) km-sized bodies, which are unknown in astronomy. The origin of these crater fields is most probably associated with secondary craters.

**High-velocity impact ejecta:** Pressure-ejecta distance from the impact crater distribution in the central cross-section of the flow after 1-km-diameter 10 km/s asteroid impact at  $45^\circ$ , reconstructed with tracers, is shown in **Fig. 2**. The source of distal solid fragments is outside the 50 GPa-isobar. The total volume of high-velocity ( $>1 \text{ km/s}$ ) solid ejecta is about  $1.5 \text{ km}^3$  (3 times the projectile volume or ~5% of total ejecta of  $\sim 30 \text{ km}^3$ ). About  $0.18 \text{ km}^3$  of these rocks have velocity above 5 km/s and probably escape Mars, creating Martian meteorites.

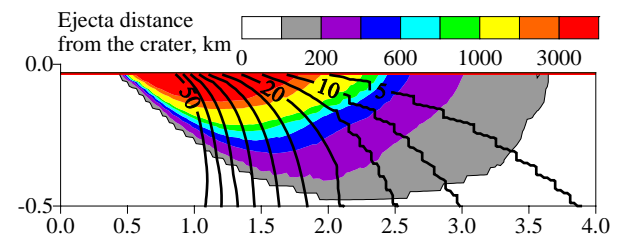


**Fig. 2** Landing site (color scale) and maximum compression (black lines with numbers) overlap corresponding to a 1-km-diameter 10 km/s asteroid impact at  $45^\circ$ . The final crater is ~10 km in diameter.

All high-velocity fragments come from the uppermost layers of the target, which is thinner than the projectile radius. The most serious problem is the size distribution of ejected fragments, as exactly this factor defines particle-gas interaction, ejecta final velocity, and the diameter of secondary crater (or martian meteorite). The most likely fragment size to occur is defined by the strain rate value at the moment of disruption [10], or alternatively, it may be connected with ejection velocity [11], or with maximum shock compression [12]. All three methods give reasonable results with the largest fragment ejected at high velocity ( $>1 \text{ km/s}$ ) of about 10 m (for the 10-km-diameter final crater). The largest fragments are from a very thin surficial layer in agreement with the spallation theory [11].

**Martian meteorites:** Numerical modeling [6] shows that escaping ejecta from moderate-size craters (~3-km-diameter according to estimates of modern flux on Mars and the variety of martian meteorites [13]) consist of fragments not larger than 1 m with maximum at 10-15 cm. Practically all fragments smaller than 10 cm are decelerated in the Martian atmosphere creating distal m-sized secondaries, while larger fragments escape Mars and can reach the Earth. The results of modeling are consistent with available petrological and geophysical data – shock metamorphism in martian meteorites [14], their burial depth [15], and pre-atmospheric size [16]. The temperature increase may be rather low, less than 100 K, for nakhlites and Chassigny.

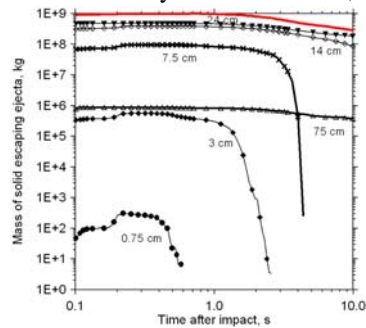


**Fig. 3** Deceleration of escape ejecta in the Martian atmosphere. Only fragments larger than 14 cm retain escape velocity in the upper atmosphere.

**Secondaries:** Our modeling of the Zunil impact event [2] produces  $10^{10}$  rock fragments  $\geq 10$  cm diameter, leading to up to  $10^9$  secondary craters  $\geq 10$  m diameter. Nearly all of the simulated secondary craters larger than 50 m are within 800 km of the impact site but the more abundant smaller (10-50 m) craters extend out to 3500 km. Clustered impacts would be most common close to the primary (due to lower ejection velocity and less time for dispersion). This finding supports the hypothesis [1] that there can be huge numbers of distant secondaries.

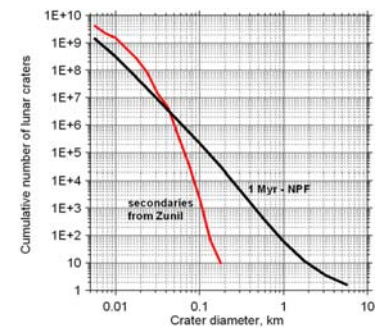
Examination of many MOC images across Mars revealed that nearly all small craters appear shallow and flat-floored. The freshest craters with sharp rims and little evidence for modification have the depth-diameter ratio of 0.11 [2] in contrast to the fresh primaries with the ratio of 0.2. This difference is usually explained through impact by clustered projectile, and/or lower impact velocity. Unfortunately, the resolution of numerical models and absence of a 3D-model with strength does not allow us to verify these assumptions.

**Size-frequency distribution – primaries versus secondaries:** The SFD of the simulated secondary craters is shown in **Fig. 4**, along with the cumulative number of Martian primary craters [17] produced globally in 1 Ma. Thus, even globally, the number of secondaries may exceed the number of primaries for craters smaller than 50 m. We also expect  $\sim 10^2$  craters

larger than 1 km, each of which would produce additional (probably substantially smaller) secondaries.

**Discussion:** Atmospheric permeability for high-velocity ejecta depends on two factors – fragment size and the scale of impact event. While the fate of m-sized fragments does not depend on atmosphere, smaller (and much more common) fragments may be decelerated even in a moderate post-impact plume (crater size less than 10 km). As the maximum fragment size decreases roughly linearly with projectile size, a rather abrupt boundary between craters with distal ejecta and without it should exist. Our modeling allows us to suggest that 2-3-km-diameter craters are the smallest ones to produce substantial fields of secondaries. A serious problem is the dispersion of high-velocity ejecta in the atmosphere and clustering of secondaries. The value of dispersion depends on the ejection velocity and its gradient as  $2V_{ej}\Delta V_{ej}/g$ , i.e. may reach tens of km for distal secondaries. At the same time a crater created by a tight or loose projectile should differ in shape from standard craters [18].

**Fig. 4.** Cumulative numbers of craters on the whole Martian surface accumulated over 1 Ma based on the Neukum production function (black line). The red line represents secondaries predicted from the Zunil-like impact simulation. The best fits are  $N \sim D^{-3.2}$  for the range 10-30 m, and  $N \sim D^{-10}$  in the range 50-150 m.



**References:** [1]. Shoemaker E.M. (1965) *The Nature of the Lunar Surface* 2, 23-77, [2] McEwen A. et al (2005) *Icarus*, in press. [3] Bierhaus E.B. et al. (2004) *LPSC* 35, abs.1963. [4] Shuvalov V. (1999) *Shock waves* 9, 381-390. [5] Pierazzo et al (2005) *GSA Special paper* 384, in press. [6] Artemieva N., Ivanov B. *Icarus* 171, 84-101 [7] Artemieva N. and Shuvalov V. (2001) *JGR* 106, 3297. [8] Bland P., Artemieva N. (2003) *Nature* 424, 288-291. [9] Chyba C. F. et al (1993) *Nature*, 361, 40. [10] Grady E.E., M.E. Kipp (1980) *Int'l. J. Rock Mech. Min. Sci. Geomech.* 17, 147-157. [11] Melosh, H.J. (1984) *Icarus* 59, 234-260. [12] Shuvalov V.V. (2002) *LPSC* 33, abs.1259. [13] Head J. N. et al. (2002) *Science* 298, 1752-1756. [14] Nyquist L. E. et al. (2001) *Space Science Reviews* 96, 105-164. [15] Mikouchi T. et al. (2003) *LPSC XXXIV*, abstract #1883. [16] Eugster O. et al. (2002) *M&PS* 37, 1345-1360. [17] Neukum G. et al. (2001) *Space Science Rev.* 96, 55-86. [18] Schultz P.H., and D.E. Gault (1985) *J. Geophys. Res.* 90, 3701-3732.